Organic & Biomolecular Chemistry

Cite this: *Org. Biomol. Chem.*, 2012, **10**, 2656

www.rsc.org/obc

PAPER

A search for BACE inhibitors reveals new biosynthetically related pyrrolidones, furanones and pyrroles from a southern Australian marine sponge, *Ianthella* sp.†

Hua Zhang,‡ Melissa M. Conte, Xiao-Cong Huang, Zeinab Khalil and Robert J. Capon*

Received 18th October 2011, Accepted 12th January 2012
DOI: 10.1039/c2ob06747a

Fractionation of a southern Australian marine sponge, *Ianthella* sp., yielded sixteen metabolites including a new class of pyrrolidone, ianthellidones A–F (**1–6**), a new class of furanone, ianthellidones G–H (**7–8**), new and known lamellarins, lamellarins O1 (**9**), O2 (**10**), O (**11**) and Q (**12**), plus the known 4-hydroxybenzaldehyde (**13**), 4-hydroxybenzoic acid (**14**), 4-methoxybenzoic acid (**15**) and ethyl 4-hydroxybenzoate (**16**). Structures for all *Ianthella* metabolites were determined by detailed spectroscopic analysis, supported by a plausible biosynthetic relationship. The ianthellidones were non-cytotoxic towards two human colon cancer cell lines (SW620 and SW620 Ad300), as well as Gram +ve and Gram −ve bacteria, and a fungus. Ianthellidone F (**6**) and lamellarins O2 (**10**) and O (**11**) displayed modest BACE inhibitory properties (IC_{50} > 10 μM), while lamellarin O1 (**9**) was more potent (IC_{50} < 10 μM). Lamellarin O (**11**) exhibited modest cytotoxicity towards SW620 and SW620 Ad300 cell lines (IC_{50} > 22 μM), was an inhibitor of the multi-drug resistance efflux pump P-glycoprotein, and displayed selective growth inhibitory activity against the Gram +ve bacterium *Bacillus subtilis* (ATCC 6633) (IC_{50} 2.5 μM).

Introduction

Neurodegenerative diseases represent a very significant burden to modern healthcare, exacerbated by heightened onset in an increasingly aging population in developed and developing countries. Sadly, effective therapeutic intervention for many neurodegenerative diseases remains limited to palliative care. The magnitude of this challenge is especially evident in diseases characterized by an amyloid plaque pathology which correlate with severely impaired cognitive ability leading to dementia (*i.e.* Alzheimer's). That other diseases share amyloid plaque pathology (*i.e.* the inflammatory muscle disease inclusion body myositis, Lewy body disease and cerebral amyloid angiopathy), raises the possibility of a common pharmaceutical target.

Of particular note, the protease β-secretase (BACE) plays a critical role in processing the essential neuronal transmembrane amyloid precursor protein (APP) to release the peptide beta-amyloid (Aβ). Since aggregation of Aβ fuels amyloid plaque pathology, a small molecule inhibitor of BACE offers the prospect of managing both Aβ and plaque levels, potentially mediating the onset and severity of the disease.

Attractive as this hypothesis is, the challenge of bringing BACE inhibitors to the clinic is not to be underestimated. Notwithstanding the challenge, the potential rewards in increased lifespan and quality of life mitigate in favor of pursuing this objective, with an important early step being the discovery of a diverse array of small molecule chemical scaffolds with BACE inhibitory properties, from which to select those that will inspire and inform future drug development.

This report describes our investigations into the chemical diversity of a unique collection of southern Australian and Antarctic marine invertebrates and algae, with the aim of detecting, isolating and identifying new BACE inhibitors. During this program we assayed ~2600 extracts for BACE inhibitory activity and used chemical profiling technologies (HPLC-DAD-MS and ^{1}H NMR) to prioritize promising hits. One particularly noteworthy hit was derived from a marine sponge, *Ianthella* sp. (CMB-01245), collected during scientific trawling operations in Bass Strait, Australia. A portion of the aqueous EtOH extract from this specimen was concentrated *in vacuo* and the residue subjected to fractionation by solvent partitioning and sequential trituration, followed by reversed-phase chromatography (SPE and HPLC), to yield an array of sixteen pure metabolites. These metabolites included six members of a new class of pyrrolidone,

Division of Chemistry and Structural Biology, Institute for Molecular Bioscience, The University of Queensland, St. Lucia, Queensland 4072, Australia. E-mail: r.capon@uq.edu.au; Fax: +61 7 3346 2090; Tel: +61 7 3346 2979

†Electronic supplementary information (ESI) available: Tabulated 1D and 2D NMR data for new compounds, along with ^{1}H NMR spectra for all compounds. See DOI: 10.1039/c2ob06747a

‡Current address: Department of Natural Medicinal Chemsitry, Shanghai Insititue of Materia Medica, Chinese Academy of Sciences, Shanghai 201203, P. R. China.

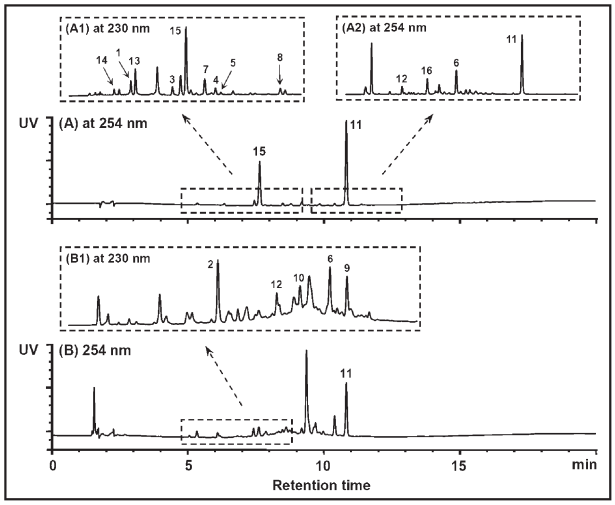

Fig. 1 C_{18} HPLC-DAD chromatograms of *Ianthella* sp. CH_2Cl_2 (**A**) and MeOH (**B**) triturations, as well as expanded chromatograms for derived SPE fractions (**A1**, **A2** and **B1**).

Table 1 ^{1}H NMR data (methanol-d_4) for ianthellidones A–E (**1–5**)

No.	1	2	3	4	5
2′/6′	7.24[a]	7.22[a]	7.27[a]	7.26[a]	7.27[a]
3′/5′	6.66[a]	6.62[a]	6.67[a]	6.67[a]	6.67[a]
2″/6″	7.20[b]	7.15[c]	7.23[b]	7.22[b]	7.23[b]
3″/5″	6.75[b]	6.77[c]	6.76[b]	6.76[b]	6.76[b]
2-CO_2**C**H_3	3.72[d]	3.68[d]	3.68[d]	3.69[d]	3.69[d]
2-OC**H**$_2$$CH_3$		4.35[e]			
2-OCH_2**C**H_3		1.36[f]			
1*N*-C**H**$_2$$OCH_3$			4.97[g]		
			4.79[g]		
1*N*-CH_2OC**H**$_3$			3.30[d]		
1*N*-C**H**$_2$$OCH_2CH_3$				5.07[g]	
				4.78[g]	
1*N*-CH_2OC**H**$_2$$CH_3$				3.59[e]	
				3.48[e]	
1*N*-CH_2OCH_2C**H**$_3$				1.15[h]	
1*N*-C**H**$_2$$CO_2$ CH_2CH_3					4.19[i]
					4.14[i]
1*N*-CH_2CO_2 C**H**$_2$$CH_3$					4.20[e]
1*N*-CH_2CO_2 CH_2C**H**$_3$					1.28[f]

[a] (d, *J* 8.9 Hz). [b] (d, *J* 8.8 Hz). [c] (d, *J* 8.7 Hz). [d] (s). [e] (m). [f] (t, *J* 7.1 Hz). [g] (d, *J* 11.2 Hz). [h] (t, *J* 7.0 Hz). [i] (d, *J* 17.7 Hz).

ianthellidones A–F (**1–6**), two members of a new class of furanone, ianthellidones G–H (**7–8**), two new and two known examples of the lamellarin class of pyrrole alkaloid, lamellarins O1 (**9**), O2 (**10**), O (**11**)[1] and Q (**12**),[2] plus the known aromatics 4-hydroxybenzaldehyde (**13**), 4-hydroxybenzoic acid (**14**), 4-methoxybenzoic acid (**15**) and ethyl 4-hydroxybenzoate (**16**). Fig. 1 illustrates a relative abundance spanning two orders of magnitude for **1–16** across key solvent triturations and chromatographic fractions (as detected against the specfied wavelength).

The structures for all sixteen *Ianthella* co-metabolites were determined by spectroscopic analysis, with a detailed account of the structure elucidation of the new metabolites **1–10** shown below. The 1D NMR (methanol-d_4) data for **1–5** is summarized in Tables 1 and 2, and **6–10** in Tables 3 and 4, with more detailed 2D NMR analysis provided in the ESI.†

Table 2 ^{13}C NMR data (methanol-d_4) for ianthellidones A–E (**1–5**)

No.	1	2	3	4	5
1′	124.1	124.5	123.7	123.7	124.0
2′/6′	131.8	131.5	131.8	131.8	131.9
3′/5′	116.3	116.3	116.4	116.4	116.4
4′	159.9	159.9	160.1	160.1	160.0
1″	123.7	123.8	123.5	123.5	123.6
2″/6″	132.2	132.1	132.2	132.2	132.2
3″/5″	116.4	116.5	116.5	116.5	116.5
4″	159.1	159.1	159.3	159.3	159.3
2	ND	98.4	89.4	89.4	90.5
3	151.9	156.6	151.2	151.2	151.1
4	131.9	131.6	131.9	131.8	131.9
5	ND	176.5	173.0	172.8	172.8
2-**C**O_2CH_3	171.9	173.0	171.4	171.4	170.9
2-CO_2**C**H_3	53.8	53.6	53.8	53.9	53.9
2-O**C**H_2CH_3		66.4			
2-OCH_2**C**H_3		14.7			
1*N*-**C**H_2OCH_3			70.8		
1*N*-CH_2O**C**H_3			56.9		
1*N*-**C**$H_2OCH_2CH_3$				69.2	
1*N*-CH_2O**C**H_2CH_3				65.4	
1*N*-CH_2OCH_2**C**H_3				15.4	
1*N*-**C**$H_2CO_2CH_2CH_3$					41.2
1*N*-CH_2**C**$O_2CH_2CH_3$					170.5
1*N*-CH_2CO_2**C**H_2CH_3					62.7
1*N*-$CH_2CO_2CH_2$**C**H_3					14.6

ND Signals not detected.

Results and discussion

High resolution ESI(+)MS analysis of **1** revealed a quasi-molecular ion $[M + Na]^+$ consistent with a molecular formula ($C_{18}H_{15}NO_6$, Δmmu 0.8) incorporating twelve double bond equivalents (DBE). Analysis of the NMR (methanol-d_4) data for **1** revealed protonated structure fragments comprising a methyl ester [δ_H 3.72 (CO_2CH_3); δ_C 171.9 (**C**O_2CH_3), 53.8 (CO_2**C**H_3)] and two para-disubstituted benzenes [benzene A: δ_H 7.24 (H-2′/6′), 6.66 (H-3′/5′); δ_C 124.1 (C-1′), 131.8 (C-2′/6′), 116.3 (C-3′/5′), 159.9 (C-4′); benzene B: δ_H 7.20 (H-2″/6″), 6.75 (H-3″/5″); δ_C 123.7 (C-1″), 132.2 (C-2″/6″), 116.4 (C-3″/5″), 159.1 (C-4″)], with deshielded resonances for C-4′ and C-4″ requiring substitution by oxygen. Further examination of the NMR data revealed a tetrasubstituted olefin [δ_C 151.9 (C-3), 131.9 (C-4)] with the highly deshielded resonance of C-3 being suggestive of a C-4 carbonyl substituent. HMBC correlations from H-2′/6′ to C-3 and H-2″/6″ to C-4 positioned the two benzene rings as indicated. The observations outlined above accounted for $C_{17}H_{11}O_5$ and eleven DBE, leaving CH_4NO incorporating one ring and four exchangeable protons. These latter observations strongly suggested that ianthellidone A (**1**) possessed the pyrrolidone moiety as shown, although the failure to detect NMR resonances for C-2 and C-5 made this assignment equivocal. Fortunately spectroscopic analysis of the co-metabolite **2** (shown below) provided definitive evidence for C-2 and C-5.

High resolution ESI(+)MS analysis of **2** revealed a quasi-molecular ion $[M + Na]^+$ consistent with a molecular formula ($C_{20}H_{19}NO_6$, Δmmu −0.4) suggestive of a +28 amu homologue of **1**. Comparison of NMR (methanol-d_4) data for **2** with **1** revealed the only significant difference being an ethoxyl moiety [δ_H 4.35 (2-OC**H**$_2$$CH_3$), 1.36 (2-$OCH_2$C**H**$_3$); δ_C 66.4

Table 3 ^{1}H NMR data (methanol-d_4) for ianthellidones F–H (**6–8**) and lamellarins O1–O2 (**9–10**)

No.	6	7	8	9	10
2′/6′	7.28[a]	7.34[b]	7.34[e]	7.00[d]	6.92[d]
3′/5′	6.67[a]	6.69[b]	6.71[e]	6.70[d]	6.69[d]
2″/6″	7.26[c]	7.25[d]	7.27[b]	6.91[b]	6.82[d]
3″/5″	6.77[c]	6.80[d]	6.81[b]	6.58[b]	6.55[d]
2‴/6‴	8.04[a]			7.95[f]	7.20[f]
3‴/5‴	7.05[a]			6.85[f]	6.76[f]
4‴-O**C**H$_3$	3.89[g]				
2-CO$_2$C**H$_3$**	3.68[g]	3.74[g]	3.74[g]	3.42[g]	3.54[g]
2-OC**H$_3$**			3.46[g]		
5				7.07[g]	6.93[g]
6	4.93[h]				
4.84[h]			5.81[g]	4.59[i]	
4.34[j]					
7					4.91[k]

[a] (d, *J* 8.9 Hz). [b] (d, *J* 8.8 Hz). [c] (d, *J* 8.7 Hz). [d] (d, *J* 8.6 Hz). [e] (d, *J* 9.0 Hz). [f] (d, *J* 8.5 Hz). [g] (s). [h] (d, *J* 17.9 Hz). [i] (dd, *J* 13.6, 4.5 Hz). [j] (dd, *J* 13.6, 8.0 Hz). [k] (dd, *J* 4.5, 8.0 Hz).

Table 4 ^{13}C NMR data (methanol-d_4) for compounds **6–10**

No.	6	7	8	9	10
1′	124.1	122.3	121.7	128.8	128.8
2′/6′	131.9	132.0	131.9	133.1	133.0
3′/5′	116.4	116.6	116.8	115.5	115.4
4′	160.1	161.1	161.5	157.3	157.3
1″	123.7	122.5	122.1	127.7	127.7
2″/6″	132.3	132.0	132.1	130.6	130.5
3″/5″	116.5	116.7	116.8	116.0	115.9
4″	159.2	159.7	160.0	156.8	156.7
1‴	129.4			127.0	134.5
2‴/6‴	131.7			132.0	128.5
3‴/5‴	115.2			117.4	116.2
4‴	165.9			167.1	158.3
4‴-O**C**H$_3$	56.3				
2	90.6	102.4	105.4	121.0	120.5
3	151.2	155.0	152.8	132.8	132.9
4	132.1	127.1	128.5	126.1	125.5
5	172.8	173.0	172.1	128.7	128.9
6	45.9			56.8	58.0
7	194.1			194.8	74.8
2-O**C**H$_3$			52.3		
2-**C**O$_2$CH$_3$	170.9	169.5	167.9	164.0	164.4
2-CO$_2$**C**H$_3$	53.9	54.2	54.2	51.1	51.2

(2-O**C**H$_2$CH$_3$), 14.7 (2-OCH$_2$**C**H$_3$)]. Of note (see above), the ^{13}C NMR data for **2** revealed resonances for both C-2 (δ_C 98.4) and C-5 (δ_C 176.5). Downfield shifts for C-3 (+4.7 ppm) and the methyl ester carbonyl (+1.1 ppm) in **2** compared to **1** were consistent with a C-2 ethoxyl *versus* hydroxyl moiety. Thus ianthellidone B (**2**) was identified as the 2-*O*-ethyl analogue of **1**.

High resolution ESI(+)MS analysis of **3** revealed a quasi-molecular ion $[M + Na]^+$ consistent with a molecular formula ($C_{20}H_{19}NO_7$, Δmmu 0.8) initially suggestive of an ethanol (C_2H_5OH) adduct of **1**. Comparison of NMR (methanol-d_4) data for **3** with **1** revealed a high level of similarity with the only significant difference being the appearance of resonances for a 1*N*-methoxymethyl moiety. This functionality was identified by diagnostic NMR resonances for an oxymethylene [δ_H 4.79/4.97 (1*N*-C**H$_2$**OCH$_3$); δ_C 70.8 (1*N*-**C**H$_2$OCH$_3$)] and a methoxyl [δ_H 3.30 (1*N*-CH$_2$OC**H$_3$**); δ_C 56.9 (1*N*-CH$_2$O**C**H$_3$)] featuring mutual HMBC correlations, which was positioned on 1*N* by HMBC correlations from 1*N*-C**H$_2$**OCH$_3$ to the flanking carbons C-2 and C-5. Thus ianthellidone C (**3**) was identified as the 1*N*-methoxymethyl analogue of **1**.

High resolution ESI(+)MS analysis of **4** revealed a quasi-molecular ion $[M + Na]^+$ consistent with a molecular formula ($C_{21}H_{21}NO_7$, Δmmu −0.7) for a +14 amu homologue of **3**. Comparison of NMR (methanol-d_4) data for **4** with **3** revealed a high level of similarity with the only significant difference being extension of the 1*N*-methoxymethyl to a 1*N*-ethoxymethyl moiety [δ_H 4.78/5.07 (1*N*-C**H$_2$**OCH$_2$CH$_3$), 3.48/3.59 (1*N*-CH$_2$OC**H$_2$**CH$_3$), 1.15 (1*N*-CH$_2$OCH$_2$C**H$_3$**); δ_C 69.2 (1*N*-**C**H$_2$OCH$_2$CH$_3$), 65.4 (1*N*-CH$_2$O**C**H$_2$CH$_3$), 15.4 (1*N*-CH$_2$OCH$_2$**C**H$_3$)]. Thus ianthellidone D (**4**) was identified as the 1*N*-ethoxymethyl analogue of **1**.

High resolution ESI(+)MS analysis of **5** revealed a quasi-molecular ion $[M + Na]^+$ consistent with a molecular formula ($C_{22}H_{21}NO_8$, Δmmu −0.8) for a +28 amu homologue of **4**. Comparison of NMR (methanol-d_4) data for **5** with **4** revealed a high level of similarity with the only significant difference being conversion of the 1*N*-ethoxymethyl to a 1*N*-CH$_2$CO$_2$Et moiety [δ_H 4.14/4.19 (1*N*-C**H$_2$**CO$_2$CH$_2$CH$_3$), 4.20 (1*N*-CH$_2$CO$_2$C**H$_2$**CH$_3$), 1.28 (1*N*-CH$_2$CO$_2$CH$_2$C**H$_3$**); δ_C 41.2 (1*N*-**C**H$_2$CO$_2$CH$_2$CH$_3$), 170.5 (1*N*-CH$_2$**C**O$_2$CH$_2$CH$_3$), 62.7 (1*N*-CH$_2$CO$_2$**C**H$_2$CH$_3$), 14.6 (1*N*-CH$_2$CO$_2$CH$_2$**C**H$_3$)]. Thus ianthellidone D (**4**) was identified as the 1*N*-CH$_2$CO$_2$Et analogue of **1**.

High resolution ESI(+)MS analysis of **6** revealed a quasi-molecular ion $[M + Na]^+$ consistent with a molecular formula ($C_{27}H_{23}NO_8$, Δmmu 0.1). Comparison of NMR (methanol-d_4) data for **6** with **5** revealed a high level of similarity with the only significant difference being centred on the 1*N* substituent. Comparison of the NMR data for **6** with the known marine sponge alkaloid and co-metabolite lamellarin O (**11**)[1] confirmed a common 1*N* substituent – namely a *para*-methoxyacetophenone moiety. Thus ianthellidone F (**6**) was assigned the structure as shown.

High resolution ESI(+)MS analysis of **7** revealed a quasi-molecular ion $[M + Na]^+$ consistent with a molecular formula ($C_{18}H_{14}O_7$, Δmmu 1.0) suggestive of a lactone (de-amino oxo) analogue of the pyrrolidone **1**. Comparison of NMR (methanol-d_4) data for **7** with those for the pyrrolidones **1–6** confirmed this hypothesis, revealing a high level of similarity where NMR differences were largely limited to a downfield shift for C-2 in **7** (δ_C 102.4) compared to **2** (δ_C 98.4), **3** (δ_C 89.4), **4** (δ_C 89.4), **5** (δ_C 90.5) and **6** (δ_C 90.6). Thus ianthellidone G (**7**) was identified as a lactone analogue of **1**.

High resolution ESI(+)MS analysis of **8** revealed a quasi-molecular ion $[M + Na]^+$ consistent with a molecular formula ($C_{19}H_{16}O_7$, Δmmu −0.6) for a +14 amu homologue of **7**. Comparison of NMR (methanol-d_4) data for **8** with **7** revealed a high level of similarity with the only significant difference being a methoxyl moiety [δ_H 3.46 (2-OC**H$_3$**); δ_C 52.3 (2-O**C**H$_3$)] with HMBC correlation to C-2 (δ_C 105.4). Thus ianthellidone H (**8**) was identified as the 2-*O*-methyl analogue of **7**.

High resolution ESI(+)MS analysis of **9** revealed a quasi-molecular ion $[M + Na]^+$ consistent with a molecular formula ($C_{26}H_{21}NO_6$, Δmmu −0.6) suggestive of a −14 amu homologue of lamellarin O (**11**).[1] Comparison of the NMR (methanol-d_4)

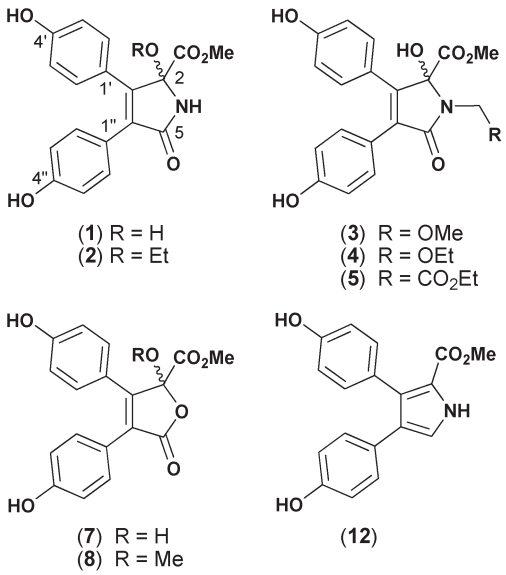

Fig. 2 *Ianthella* sp. (CMB-01245) metabolites **1–8** and **12**.

data for **9** with those for **11** revealed a high level of similarity, inclusive of a 2-CO_2Me moiety (δ_H 3.42, 2-$CO_2C\mathbf{H}_3$; δ_C 51.1, 2-$CO_2\mathbf{C}H_3$ and 164.0, 2-$\mathbf{C}O_2CH_3$), with the only significant differences being centred around C-4‴ consistent with a 4‴-OH moiety. Thus lamellarin O1 (**9**) was identified as the 4‴-*O*-demethyl analogue of lamellarin O (**11**).

High resolution ESI(+)MS analysis of **10** revealed a quasi-molecular ion $[M + Na]^+$ consistent with a molecular formula ($C_{26}H_{23}NO_6$, Δmmu −0.7) suggestive of a dihydro analogue of **9**. Comparison of the NMR (methanol-d_4) data for **10** with those for **9** revealed a high level of similarity, with the only difference being attributed to reduction of the C-7 keto in **9** to a C-7 hydroxyl in **10** [δ_H 4.59/4.34 (H_2-6), 4.91 (H-7); δ_C 58.0, (C-6), 74.8 (C-7)]. Thus lamellarin O2 (**10**) was identified as the C-7 hydroxyl analogue of lamellarin O1 (**9**).

All the ianthellidones A–H (**1–8**) incorporate a single chiral centre and exhibit no measureable optical rotation, indicating they are racemic. The very close structural similarity between the ianthellidones **1–8** and the lamellarins **9–12** suggests a common biosynthetic origin, leading us to hypothesize that the ianthellidone pyrrolidone ring system is formed *via* oxygen addition across the lamellarin pyrrole moiety, as illustrated in Fig. 3 (**12** to **1**, and **11** to **6**). In this process the regiochemistry of the endo peroxide ring opening is driven by the need to abstract a flanking proton (H-5) in a system where C-2 is fully substituted. Subsequent elimination of H_2O from ianthellidone A (**1**) would return an imine that could be quenched by H_2O to reform **1**, or EtOH to yield ianthellidone B (**2**) (Fig. 2). By contrast, as ianthellidones C–F (**3–6**) are 1*N*-substituted the elimination of H_2O is disfavoured, rendering these metabolites immune to solvolysis during storage or handling. While the methoxymethyl (MOM) moiety in **3** is well known as a protecting group in synthetic organic chemistry, it is rare in natural products,[3–6] and even rarer still when incorporated into an amide.[7–9] The ethoxymethyl amide moiety in **4** seems likely to be a solvolysis artifact induced by prolonged storage of **3** in EtOH, whereas the ethyl ester **5** is in all probability derived from ethanolysis of a suitable

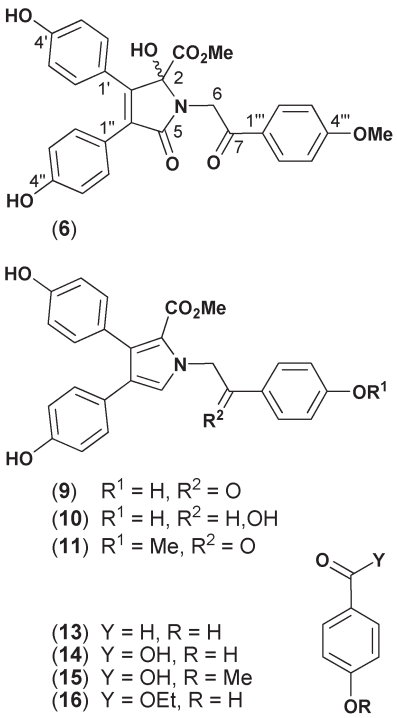

Fig. 3 *Ianthella* sp. (CMB-01245) metabolites **9–10**, **13–16** and **6**.

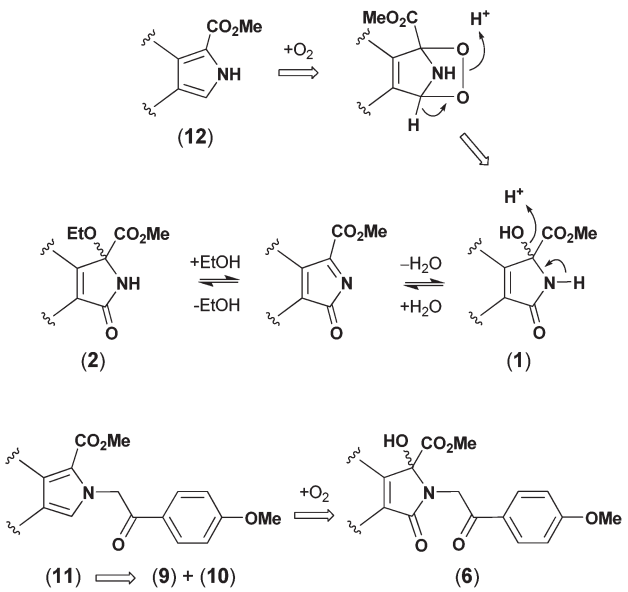

Fig. 4 Plausible biosynthetic relationships between lamellarins and ianthellidones.

(unisolated) acid precursor. The furanones **7** and **8** are likely derived from hydrolysis and ring opening of the pyrrolidone **1** with concomitant ring closure and deamination. That all of **1–8** are racemic suggests a non-stereoselective oxygen addition across the pyrrole biosynthetic precursor (Fig. 4).

On investigating the *in vitro* BACE inhibitory properties of co-metabolites **1–16** (at 10 μM) we noted a reduction in BACE activity for lamellarin O1 (**9**) (60%), with lesser degrees of inhibition for ianthellidone F (**6**) (40%), lamellarin O2 (**10**) (40%)

and lamellarin O (**11**) (40%). While these levels of BACE inhibition are modest, they nevertheless reveal the ianthellidones and lamellarins as potential BACE inhibitory scaffolds.

Extending our biological investigations we established that lamellarin O (**11**) displayed weak cytotoxicity (IC_{50} > 22 μM) when tested in a cell viability assay against a human colon cancer cell line (SW620) and a multi-drug resistant (P-glycoprotein over expressing) derived cell line (SW620 Ad300), while the remaining co-metabolites were not cytotoxic (IC_{50} > 30 μM) in these assays. In a corollary experiment we determined that **11** (at 20 μM) exerted a 58% inhibition of the multi-drug resistance efflux pump P-glycoprotein, compared to the inhibitory effect of the positive control verapamil (at 100 μM). Likewise, whereas **11** displayed significant growth inhibitory activity against the Gram positive bacterium *Bacillus subtilis* (ATCC 6633) (MIC 15 μM), neither **11** nor the remaining co-metabolites **1–10** or **12** exhibited inhibitory activity (MIC > 20 μM) against the fungus *Candida albicans* (ATCC 90028), the Gram-negative bacterium *Escherichia coli* (ATCC 11775), or the Gram-positive bacteria *Staphylococcus aureus* (ATCC 9144 and ATCC 25923) and *Bacillus subtilis* (ATCC 6051).

The observations made above notwithstanding, we note that the dominant BACE inhibitory activity of the *Ianthella* sp. (CMB-01245) extract was traced to fractions that chemical profiling revealed to be a complex unresolved mixture of non-ianthellidone and non-lamellarin alkaloids. These fractions are the subject of separate investigations and the identity and biological properties of the associated BACE inhibitory agents will be reported at a later date.

Conclusions

In conclusion, our investigations into *Ianthella* sp. (CMB-01245) have returned an unprecedented class of pyrrolidones (**1–6**) and furanones (**7–8**), plus new (**9–10**) and known (**11–12**) lamellarins. Structures were assigned to the new metabolite **1–10** on the basis of detailed spectroscopic analysis, further informed by biosynthetic considerations. The ianthellidones (**1–8**) displayed low to no cytotoxicity when measured in a range of assays against mammalian (human), bacterial and fungal cells. Lamellarin O1 (**9**) displayed noteworthy BACE inhibitory activity. The low natural abundance of ianthellidones (0.05 to 0.79%) may explain how this molecular motif remained undetected for so long, despite intensive exploratory efforts of marine natural products chemists over several decades. Given limited access to natural supplies, future biological evaluation of the ianthellidone scaffold will likely be dependent on total synthesis. In this regard the proposed biosynthetic link between the ianthellidones and lamellarins suggests an attractive biomimetic strategy.

Experimental section

General experimental procedures

Optical rotations were measured on a JASCO P-1010 polarimeter with a 10 cm length cell. UV spectra were obtained on a Cary 50 UV-visible spectrophotometer with 1 cm pathway cell. NMR experiments were performed on a Bruker Avance DRX600 spectrometer and are referenced to residual ^1H signals in the deuterated solvents. ESIMS experiments were carried out on an Agilent 1100 series LC/MSD (quadrupole). HR-ESIMS data were acquired on a Bruker micrOTOF mass spectrometer by direct infusion in MeCN at 3 μL min^{-1} using sodium formate clusters as an internal calibrant. All HPLC analyses and purifications were performed on Agilent 1100 series LC instruments with corresponding detectors, collectors and software. All chemicals were purchased from Merck, Sigma-Aldrich or Fluka. Solvents used for general purposes were of at least analytical grade, and solvents used for HPLC were of HPLC grade. Agilent Zorbax SB-C_{18} (5 μm, 4.6 × 150 mm (analytical) and 9.4 × 250 mm (semi-preparative)) columns were used for HPLC analyses and separations. An Alltech Extract-Clean 5 g C_{18} cartridge was used for crude fractionation.

Animal material (collection and taxonomy)

The sponge CMB-01245 was collected in May 1991 during a scientific trawling expedition in Bass Strait, Australia, aboard the RV Franklin. A description of the sponge was as follows: Growth form stalked, biplanar, anastomosing branches 5–10 mm thick; colour on deck and in EtOH dark green-black, probable aerophobic colour change; texture soft and flexible in life, light but tough and fibrous once preserved in EtOH; oscules 1–2 mm diameter, sunken between conules; surface opaque, membranous, conulose, fibre reticulation visible at the surface; spicules none; ectosome collagenous with fibre tips protruding; choanosome a rectangular reticulation of thick spongin fibres 50–100 μm in diameter, branched and anastomosing, laminated, secondary connecting fibres slightly smaller. Light collagen in the mesohyl filled with green pigment granules. Choanocyte chambers eurypylous.

Based on this analysis the sponge CMB-01245 was identified as an *Ianthella* sp. (Order Verongida, Family Ianthellidae; Museum Victoria Registry No. MVF167496).

Extraction, fractionation and isolation

A portion (*ca.* 180 mL) of the EtOH extract of *Ianthella* sp. (CMB-01245) was decanted and concentrated *in vacuo* to return a black solid (1.87 g), which was subsequently partitioned into *n*-BuOH (2 × 40 mL) and H_2O (50 mL) solubles. Bioassay analysis localized the BACE inhibitory activity in the *n*-BuOH solubles (739 mg). The *n*-BuOH partition was sequentially triturated with *n*-hexane (3 × 10 mL), CH_2Cl_2 (3 × 10 mL) and MeOH (5 mL), and each solvent trituration was concentrated *in vacuo* to yield *n*-hexane (36 mg), CH_2Cl_2 (189 mg) and MeOH (402 mg) soluble fractions.

The CH_2Cl_2 soluble fraction (189 mg) was eluted through an Alltech C_{18} SPE cartridge using a 10 mL 10% stepwise gradient elution from 30% MeOH–H_2O to 100% MeOH, and the elutions were combined based on HPLC analyses to return six fractions. The first fraction was fractionated by a Zorbax SB-C_{18} semi-preparative column (4.0 mL min^{-1}, 20 min gradient elution from 80% H_2O–MeCN to 60% H_2O–MeCN with a constant 0.01% TFA) to produce in sequence 4-hydroxybenzoic acid (**14**, 0.5 mg), ianthellidone A (**1**, 0.6 mg), 4-hydroxybenzaldehyde

(**13**, 0.9 mg), ianthellidone C (**3**, 0.6 mg), 4-methoxybenzoic acid (**15**, 5.4 mg), ianthellidone G (**7**, 0.6 mg), ianthellidone D (**4**, 0.7 mg), ianthellidone E (**5**, 0.4 mg) and ianthellidone H (**8**, 0.6 mg). The second fraction (18.0 mg) was fractionated by a Zorbax SB-C_{18} semi-preparative column (4.0 mL min^{-1}, 15 min gradient elution from 70% H_2O–MeCN to 55% H_2O–MeCN with a constant 0.01% TFA, followed by a 1 min ramp to 40% H_2O–MeCN followed by a 4 min hold) to yield sequentially lamellarin Q (**12**, 0.9 mg), ethyl 4-hydroxybenzoate (**16**, 0.5 mg), ianthellidone F (**6**, 2.0 mg) and lamellarin O (**11**, 2.3 mg). The third fraction was pure and was identified as lamellarin O (**11**, 26.8 mg).

A portion of the MeOH solubles (116 mg) was eluted through an Alltech C_{18} SPE cartridge using a stepwise gradient elution (as above) to return five fractions. The second fraction (38.9 mg) was fractionated by a Zorbax SB-C_{18} semi-preparative column (4.0 mL min^{-1}, 15 min 75% H_2O–MeCN to 50% H_2O–MeCN gradient elution) to yield in sequence ianthellidone B (**2**, 1.4 mg), lamellarin Q (**12**, 0.6 mg), lamellarin O2 (**10**, 0.6 mg), ianthellidone F (**6**, 1.1 mg), lamellarin O1 (**9**, 0.9 mg) and lamellarin O (**11**, 0.5 mg).

Yields estimated as a weight to weight % against the *n*-BuOH partition (739 mg) are as *follows*; ianthellidone A (**1**, 0.08%), ianthellidone B (**2**, 0.66%), ianthellidone C (**3**, 0.08%), ianthellidone D (**4**, 0.09%), ianthellidone E (**5**, 0.05%), ianthellidone F (**6**, 0.79%), ianthellidone G (**7**, 0.08%), ianthellidone H (**8**, 0.08%), lamellarin O1 (**9**, 0.42%), lamellarin O2 (**10**, 0.28%) lamellarin O (**11**, 4.2%), lamellarin Q (**12**, 0.41%), 4-hydroxybenzaldehyde (**13**, 0.12%), 4-hydroxybenzoic acid (**14**, 0.07%), 4-methoxybenzoic acid (**15**, 0.73%) and ethyl 4-hydroxybenzoate (**16**, 0.07%).

Ianthellidone A (1). Off-white solid; $[\alpha]_D^{22}$ −0.1 (*c* 0.06, MeOH); UV (MeOH) λ_{max} (log ε) 234 (4.07), 287 (3.80) and 325 (3.77) nm; ^1H and ^{13}C NMR (methanol-d_4, 600 MHz) Tables 1 and 2; ESI(+)MS *m/z* 342 $[M + H]^+$, 705 $[2M + Na]^+$, ESI(−)MS *m/z* 340 $[M - H]^-$; HRESI(+)MS *m/z* 364.0784 $[M + Na]^+$ (calcd for $C_{18}H_{15}NO_6Na$, 364.0792).

Ianthellidone B (2). Off-white solid; $[\alpha]_D^{23}$ −2.0 (*c* 0.04, MeOH); UV (MeOH) λ_{max} (log ε) 231 (4.26), 288 (3.92) and 330 (3.96) nm; ^1H and ^{13}C NMR (methanol-d_4, 600 MHz) Tables 1 and 2; ESI(+)MS *m/z* 370 $[M + H]^+$, 761 $[2M + Na]^+$, ESI(−)MS *m/z* 368 $[M - H]^-$; HRESI(+)MS *m/z* 392.1109 $[M + Na]^+$ (calcd for $C_{20}H_{19}NO_6Na$, 392.1105).

Ianthellidone C (3). Off-white solid; $[\alpha]_D^{22}$ +3.6 (*c* 0.06, MeOH); UV (MeOH) λ_{max} (log ε) 239 (3.91), 288 (3.68) and 332 (3.59) nm; ^1H and ^{13}C NMR (methanol-d_4, 600 MHz) Tables 1 and 2; ESI(+)MS *m/z* 793 $[2M + Na]^+$, ESI(−)MS *m/z* 384 $[M - H]^-$; HRESI(+)MS *m/z* 408.1046 $[M + Na]^+$ (calcd for $C_{20}H_{19}NO_7Na$, 408.1054).

Ianthellidone D (4). Off-white solid; $[\alpha]_D^{22}$ +0.3 (*c* 0.06, MeOH); UV (MeOH) λ_{max} (log ε) 238 (3.90), 288 (3.66) and 333 (3.62) nm; ^1H and ^{13}C NMR (methanol-d_4, 600 MHz) Tables 1 and 2; ESI(+)MS *m/z* 821 $[2M + Na]^+$, ESI(−)MS *m/z* 398 $[M - H]^-$; HRESI(+)MS *m/z* 422.1217 $[M + Na]^+$ (calcd for $C_{21}H_{21}NO_7Na$, 422.1210).

Ianthellidone E (5). Off-white solid; $[\alpha]_D^{22}$ +2.0 (*c* 0.04, MeOH); UV (MeOH) λ_{max} (log ε) 238 (4.05), 288 (3.81) and 332 (3.74) nm; ^1H and ^{13}C NMR (methanol-d_4, 600 MHz) Tables 1 and 2; ESI(+)MS *m/z* 877 $[2M + Na]^+$, ESI(−)MS *m/z* 426 $[M - H]^-$; HRESI(+)MS *m/z* 450.1167 $[M + Na]^+$ (calcd for $C_{22}H_{21}NO_8Na$, 450.1159).

Ianthellidone F (6). Off-white solid; $[\alpha]_D^{23}$ +1.3 (*c* 0.06, MeOH);UV (MeOH) λ_{max} (log ε) 222 (4.34), 279 (4.35) and 332 (3.97) nm; ^1H and ^{13}C NMR (methanol-d_4, 600 MHz) Tables 1 and 2; ESI(+)MS *m/z* 1001 $[2M + Na]^+$, ESI(−)MS *m/z* 488 $[M - H]^-$; HRESI(+)MS *m/z* 512.1315 $[M + Na]^+$ (calcd for $C_{27}H_{23}NO_8Na$, 512.1316).

Ianthellidone G (7). Off-white solid; $[\alpha]_D^{22}$ +0.8 (*c* 0.06, MeOH); UV (MeOH) λ_{max} (log ε) 234 (3.94), 288 (3.77) and 334 (3.79) nm; ^1H and ^{13}C NMR (methanol-d_4, 600 MHz) Tables 1 and 2; ESI(+)MS *m/z* 343 $[M + H]^+$, 707 $[2M + Na]^+$, ESI(−)MS *m/z* 341 $[M - H]^-$; HRESI(+)MS *m/z* 365.0622 $[M + Na]^+$ (calcd for $C_{18}H_{14}O_7Na$, 365.0632).

Ianthellidone H (8). Off-white solid; $[\alpha]_D^{22}$ −0.5 (*c* 0.06, MeOH); UV (MeOH) λ_{max} (log ε) 235 (3.85), 291(3.66) and 341 (3.72) nm; ^1H and ^{13}C NMR (methanol-d_4, 600 MHz) Tables 1 and 2; ESI(+)MS *m/z* 357 $[M + H]^+$, 735 $[2M + Na]^+$, ESI(−)MS *m/z* 355 $[M - H]^-$; HRESI(+)MS *m/z* 379.0794 $[M + Na]^+$ (calcd for $C_{19}H_{16}O_7Na$, 379.0788).

Lamellarin O1 (9). Off-white solid; UV (MeOH) λ_{max} (log ε) 223 (4.40) and 280 (4.45) nm; ^1H and ^{13}C NMR (methanol-d_4, 600 MHz) Tables 1 and 2; ESI(+)MS *m/z* 444 $[M + H]^+$, 909 $[2M + Na]^+$, ESI(−)MS *m/z* 442 $[M - H]^-$; HRESI(+)MS *m/z* 466.1267 $[M + Na]^+$ (calcd for $C_{26}H_{21}NO_6Na$, 466.1261).

Lamellarin O2 (10). Off-white solid; $[\alpha]_D^{23}$ +0.3 (*c* 0.03, MeOH);UV (MeOH) λ_{max} (log ε) 227 (4.26), 250 (4.18) and 283 (4.03) nm; ^1H and ^{13}C NMR (methanol-d_4, 600 MHz) Tables 1 and 2; ESI(+)MS *m/z* 428 $[M - H_2O + H]^+$, 446 $[M + H]^+$, ESI(−)MS *m/z* 444 $[M - H]^-$; HRESI(+)MS *m/z* 468.1425 $[M + Na]^+$ (calcd for $C_{26}H_{23}NO_6Na$, 468.1418).

Bioassays

BACE1 assay

The TruPoint Beta-Secretase Assay was conducted according to manufacturer's instructions (Perkin Elmer, AD0258). Briefly, compounds of interest were dispensed in duplicate into a 384 well plate at the desired concentrations (7% DMSO). BACE (0.3 mU μL^{-1}; Invitrogen, P2947) was added before incubating the plate at room temperature for 30 min. The reaction was started by the addition of substrate (200 nmol L^{-1}) to a final assay volume of 30 µL. The assay plate was incubated for 24 hours at room temperature, protected from light and covered with parafilm to prevent evaporation. The assay was read at 340/615 nm using an Envision plate reader. Concentrations given are for final assay conditions.

Antibacterial assay

The bacterium to be tested was streaked onto a tryptic soy agar plate and was incubated at 37 °C for 24 hours. One colony was then transferred to fresh tryptic soy broth (15 mL) and the cell density was adjusted to 10^4–10^5 cfu mL^{-1}. Test compounds were dissolved in DMSO and diluted with H_2O to give a 300 μM stock solution (10% DMSO). The stock solution was then serially diluted with 10% DMSO to give final concentrations of 30 μM to 0.01 μM in 1% DMSO. An aliquot (20 μL) of each dilution was transferred to a 96-well microtitre plate and freshly prepared microbial broth (180 μL) was added to each well. The plates were incubated at 37 °C for 24 hours and the optical density of each well was measured spectrophotometrically at 600 nm. Each test compound was screened against the Gram-negative bacterium *Escherichia coli* (ATCC 11775), and the Gram-positive bacteria *Staphylococcus aureus* (ATCC 9144 and ATCC 25923) and *Bacillus subtilis* (ATCC 6633 and ATCC 6051).

Antifungal assay

The fungus to be tested was streaked onto a Sabouraud agar plate and was incubated at 26.5 °C for 48 hours. One colony was then transferred to fresh Sabouraud broth (15 mL) and the cell density was adjusted to 10^4–10^5 cfu mL^{-1}. Test compounds were dissolved in DMSO and diluted with H_2O to give a 300 μM stock solution (10% DMSO). The stock solution was then serially diluted with 10% DMSO to give final concentrations of 30 μM to 0.01 μM in 1% DMSO. An aliquot (20 μL) of each dilution was transferred to a 96-well microtitre plate and freshly prepared microbial broth (180 μL) was added to each well. The plates were incubated at 26.5 °C for 48 hours and the optical density of each well was measured spectrophotometrically at 600 nm. Each test compound was screened against the fungi *Candida albicans* (ATCC 90028).

Cell lines and cell culture

The parental cell line SW620 (American Type Culture Collection, Manassasm VA, CCL-227), is a human colon cell line that was originated from a lymph node metastasis in the patient with primary adenocarcinoma of the colon. The multi-drug resistant (MDR) cell line, SW620 Ad300, which over-expresses Permeable-glycoprotein (P-gp), was selected from SW620 by growth in the presence of increasing concentrations of doxorubicin. SW620 and SW620 Ad300 were grown in RPMI medium 1640 as adherent mono-layer in flasks supplemented with 10% foetal bovine serum, 2 mM L-glutamine, 100 unit mL^{-1} penicillin and 100 μg mL^{-1} streptomycin in a humidified incubator containing of 5% CO_2 at 37 °C. After SW620 Ad300 exhibited stable phenotype of P-gp, the cells were maintained in 300 ng mL^{-1} doxorubicin.

MTT cytotoxicity assay

The MTT assay was used to evaluate the cytotoxicity of compounds against cancer cell. This assay was modified slightly from that previously described.[10] Briefly, cells (2000 per well in 180 μL of RPMI 1640 supplemented with 10% FBS) were seeded evenly in a 96-well micro-plate, and the plate was incubated for 18 hours (37 °C; 5% CO_2) to allow cells to attach. Compounds to be tested were dissolved in 5% DMSO (v/v) and diluted from 300 μM-300 nM. Aliquots (20 μL) of each dilution (or of 5% aqueous DMSO for control wells) were added to the plate in duplicate. After 68 hours of incubation (37 °C; 5% CO_2), a solution of 3-(4,5-dimethylthiazol-2-yl)-2,5-diphenyltetrazolium bromide (MTT; Sigma, USA) in PBS was added to each well to a final concentration of 0.4 mg mL^{-1} and the plate was incubated for a further 4 hours (37 °C; 5% CO_2). After that, medium was carefully aspirated and precipitated formazan crystals were dissolved in DMSO (100 μL per well). Finally, the absorbance of each well at 580 nm was measured with a PowerWave XS Microplate Reader from Bio-Tek Instruments Inc. (Vinooski, VT). The IC_{50} value was calculated as the concentration of the compound required for 50% inhibition of the cancer cells using Prism 5.0 from GraphPad Software Inc. (La Jolla, CA).

Calcein AM assay (P-gp inhibitor assay)

The P-gp inhibitor assay was modified based on the literature described previously.[11] Briefly, cells that overexpress P-gp (SW620 Ad300) were harvested with trypsin and resuspended in RPMI 1640 to give a final concentration of 50×10^4 cells mL^{-1}. Cells (100 μL per well) were then plated in a 96-well, flat clear-bottom and black-well micro-plate (353219, BD Falcon, NJ) and incubated at 37 °C in 5% CO_2. After 48 hours, each well was washed twice and replaced with 50 μL warm RPMI 1640 (without phenol red). Subsequently, compounds (final concentration 20 μM), verapamil (final concentration 100 μM, positive control) or PBS (negative control and background) were distributed to designated wells (25 μL per well) in duplicate and incubated at 37 °C in 5% CO_2. 15 min later, 25 μL calcein acetoxymethyl ester (calcein AM, final concentration 0.25 μM) was added to each well except the background well which was added with 25 μL PBS. The plate was then incubated at 37 °C 5% CO_2 for a further 30 min, after which fluorescence from accumulated intracellular calcein was detected using a POLARstar Omega plate (BMG LABTECH, Offenburg, Germany) reader at an excitation wavelength of 490 nm and emission of 510 nm. Data were analysed by Prism 5.0 from GraphPad Software Inc. (La Jolla, CA).

Inhibition was evaluated using the following equation: % maximum = $(RFU_{compound} - RFU_{negative})/(RFU_{verapamil} - RFU_{negative}) \times 100$, where $RFU_{compound}$ is fluorescence in the presence of compound (20 μM), $RFU_{verapamil}$ is fluorescence in the presence of verapamil (100 μM) and $RFU_{negative}$ is fluorescence in the presence of PBS. A compound was determined to inhibit P-gp when % maximum was >30%.

Acknowledgements

The authors thank L. Goudie (Museum Victoria) for sponge taxonomy, the industry partner Noscira for initial BACE assays on crude extracts, S. Bates and R. Robey (NCI) for providing the SW620 and SW620 Ad300 cell lines, and A. Piggot (IMB, UQ)

for the acquisition of HRESIMS data. ZK and XH acknowledge financial support from The University of Queensland (UQ/IMB postgraduate award). This research was funded in part by the Institute for Molecular Bioscience, The University of Queensland and the Australian Research Council (LP0775547).

References

1 S. Urban, M. S. Butler and R. J. Capon, *Aust. J. Chem.*, 1994, **47**, 1919–1924.
2 S. Urban, L. Hobbs, J. N. A. Hooper and R. J. Capon, *Aust. J. Chem.*, 1995, **48**, 1491–1494.
3 D. Naidoo, P. H. Coombes, D. A. Mulholland, N. R. Crouch and A. J. J. van den Bergh, *Phytochemistry*, 2005, **66**, 1724–1728.
4 Y. Wu, M. Suehiro, M. Kitajima, T. Matsuzaki, S. Hashimoto, M. Nagaoka, R. Zhang and H. Takayama, *J. Nat. Prod.*, 2009, **72**, 204–209.
5 F. Wang, F.-C. Ren and J.-K. Liu, *Phytochemistry*, 2009, **70**, 650–654.
6 L. Du, X. Yang, T. Zhu, F. Wang, X. Xiao, H. Park and Q. Gu, *Chem. Pharm. Bull.*, 2009, **57**, 873–876.
7 T. Iwagawa, M. Kaneko, H. Okamura, M. Nakatani and R. W. M. van Soest, *J. Nat. Prod.*, 1998, **61**, 1310–1312.
8 A. Umeyama, S. Ito, E. Yuasa, S. Arihara and T. Yamada, *J. Nat. Prod.*, 1998, **61**, 1433–1434.
9 A. Aiello, M. D'Esposito, E. Fattorusso, M. Menna, W. E. G. Muller, S. Perovic-Ottstadt and H. C. Schroder, *Bioorg. Med. Chem.*, 2006, **14**, 17–24.
10 J. Carmichael, W. G. DeGraff, A. F. Gazdar, J. D. Minna and J. B. Mitchell, *Cancer Res.*, 1987, **47**, 943–946.
11 F. Tiberghien and F. Loor, *Anti-Cancer Drugs*, 1996, **7**, 568–578.